This is a preproof accepted article for *Mineralogical Magazine*
This version may be subject to change during the production process
DOI: 10.1180/mgm.2026.10218

New arsenate minerals from the Arsenatnaya fumarole, Tolbachik volcano, Kamchatka, Russia. XXII. Magnesiohatertite, $NaNaCa(MgFe^{3+})(AsO_4)_3$, a member of the alluaudite group

Igor V. Pekov[1]*, Inna Lykova[1], Natalia N. Koshlyakova[1], Dmitry I. Belakovskiy[2], Marina F. Vigasina[1], Atali A. Agakhanov[2], Sergey N. Britvin[3], Anna G. Turchkova[1], Leonid P. Anikin[4], Evgeny G. Sidorov[4†] and Gerald Giester[5]

[1]Faculty of Geology, Moscow State University, Vorobievy Gory, 119991 Moscow, Russia

[2]Fersman Mineralogical Museum of the Russian Academy of Sciences, Leninsky Prospekt 18-2, 119071 Moscow, Russia

[3]St. Petersburg State University, University Emb. 7/9, 199034 St. Petersburg, Russia

[4]Institute of Volcanology and Seismology, Far Eastern Branch of Russian Academy of Sciences, Piip Boulevard 9, 683006 Petropavlovsk-Kamchatsky, Russia

[5]Institute of Mineralogy and Crystallography, University of Vienna, Althanstrasse 14 (UZA 2), A-1090 Vienna, Austria

*E-mail: igorpekov@mail.ru

† Deceased 20 March 2021

Running title: Magnesiohatertite, a new mineral

Abstract

The new alluaudite-group mineral magnesiohatertite was found in the Arsenatnaya fumarole, Second scoria cone of the Northern Breakthrough of the Great Tolbachik Fissure Eruption, Tolbachik volcano, Kamchatka, Russia. It is associated with sanidine, fluorophlogopite, hematite, tenorite, cassiterite, pseudobrookite, rutile, johillerite, nickenichite, badalovite, calciojohillerite, bradaczekite, tilasite, svabite, urusovite, lammerite, paralammerite, ericlaxmanite, popovite, arsmirandite, lehmannite, arsenowagnerite, dmisokolovite, shchurovskyite, yurmarinite, aphthitalite, belomarinaite, metathénardite, langbeinite, calciolangbeinite, anhydrite, krasheninnikovite, euchlorine, wulffite, alumoklyuchevskite, fluoborite, sylvite, halite, and sellaite. Magnesiohatertite occurs as prismatic or tabular crystals up to 2 mm × 0.5 mm. They are usually combined in near-parallel or chaotic aggregates up to 0.5 cm across or form interrupted incrustations up to several cm^2 in area. Magnesiohatertite is transparent or semitransparent, with vitreous lustre. It is grey, greenish-,

Prepublished article

https://doi.org/10.1180/mgm.2026.10218 Published online by Cambridge University Press

brownish- or bluish-grey, pale blue or colourless. The mineral is brittle, cleavage was not observed. The Mohs hardness is 3½. D_{calc} is 4.060 g cm^{-3}. Magnesiohatertite is optically biaxial (+), α = 1.728(5), β = 1.745(6), γ = 1.768(6), $2V_{meas}$ = 85(10)º.The chemical composition (wt.%, electron-microprobe; holotype) is: Na_2O 7.76, K_2O 1.25, CaO 9.84, MgO 5.93, MnO 0.70, CuO 6.78, ZnO 2.85, Al_2O_3 0.64, Fe_2O_3 6.76, TiO_2 0.02, SiO_2 0.25, P_2O_5 0.25, V_2O_5 0.10, As_2O_5 56.71, SO_3 0.02, total 99.86. The empirical formula calculated based on 12 O *apfu* is $Na_{1.51}K_{0.16}Ca_{1.06}Mg_{0.89}Mn_{0.06}Cu_{0.51}Zn_{0.21}Al_{0.08}Fe^{3+}_{0.51}(As_{2.97}Si_{0.03}P_{0.02}V_{0.01})_{\Sigma 3.03}O_{12}$. Magnesiohatertite is monoclinic, *C*2/*c*, *a* = 12.3098(10), *b* = 13.0021(11), *c* = 6.7211(5) Å, β = 113.823(4)º, *V* = 984.08(14) Å^3, and *Z* = 4. The crystal structure was solved from single-crystal X-ray diffraction data and was refined to *R*1 = 0.0332. Magnesiohatertite is isostructural with other alluaudite-group minerals. Its simplified crystal chemical formula is $^{A(1)}Na^{A(2)'}Na^{M(1)}Ca^{M(2)}(MgFe^{3+})(^{T}AsO_4)_3$. The idealized formula is, according to the current nomenclature of alluaudite-group minerals, $NaNaCa(MgFe^{3+})(AsO_4)_3$. The mineral is named as a Mg-dominant analogue of hatertite, ideally $NaNaCa(CuFe^{3+})(AsO_4)_3$.

Keywords: magnesiohatertite, new mineral, alluaudite group, arsenate, crystal structure, fumarole sublimate, Tolbachik volcano, Kamchatka.

Introduction

This paper continues the description of new arsenate mineral species found in the Arsenatnaya fumarole situated at the apical part of the Second scoria cone of the Northern Breakthrough of the Great Tolbachik Fissure Eruption 1975–1976 (NB GTFE), Tolbachik volcano, Kamchatka Peninsula, Far-Eastern Region, Russia (55°41'N 160°14'E, 1200 m a.s.l.). Twenty four new minerals were characterized in the previous paper of the series: yurmarinite $Na_7(Fe^{3+},Mg,Cu)_4(AsO_4)_6$ (Pekov *et al.*, 2014a), two polymorphs of $Cu_4O(AsO_4)_2$, ericlaxmanite and kozyrevskite (Pekov *et al.*, 2014b), popovite $Cu_5O_2(AsO_4)_2$ (Pekov *et al.*, 2015a), structurally related shchurovskyite $K_2CaCu_6O_2(AsO_4)_4$ and dmisokolovite $K_3Cu_5AlO_2(AsO_4)_4$ (Pekov *et al.*, 2015b), katiarsite $KTiO(AsO_4)$ (Pekov *et al.*, 2016a), melanarsite $K_3Cu_7Fe^{3+}O_4(AsO_4)_4$ (Pekov *et al.*, 2016b), pharmazincite $KZnAsO_4$ (Pekov *et al.*, 2017), arsenowagnerite $Mg_2(AsO_4)F$ (Pekov *et al.*, 2018b), arsenatrotitanite $NaTiO(AsO_4)$ (Pekov *et al.*, 2019a), the two isostructural minerals edtollite $K_2NaCu_5Fe^{3+}O_2(AsO_4)_4$ and alumoedtollite $K_2NaCu_5AlO_2(AsO_4)_4$ (Pekov *et al.*, 2019b), anatolyite $Na_6(Ca,Na)(Mg,Fe^{3+})_3Al(AsO_4)_6$ (Pekov *et al.*, 2019c), zubkovaite $Ca_3Cu_3(AsO_4)_4$ (Pekov *et al.*, 2019d), pansnerite $K_3Na_3Fe^{3+}_6(AsO_4)_8$ (Pekov *et al.*, 2020a), badalovite

Prepublished article

https://doi.org/10.1180/mgm.2026.10218 Published online by Cambridge University Press

$NaNaMg(MgFe^{3+})(AsO_4)_3$ (Pekov *et al.*, 2020b), calciojohillerite $NaCaMgMg_2(AsO_4)_3$ (Pekov *et al.*, 2021a), yurgensonite $K_2SnTiO_2(AsO_4)_2$ (Pekov *et al.*, 2021b), paraberzeliite $NaCaCaMg_2(AsO_4)_3$ (Pekov *et al.*, 2022a), khrenovite $Na_3Fe^{3+}{}_2(AsO_4)_3$ (Pekov *et al.*, 2022b), axelite $Na_{14}Cu_7(AsO_4)_8F_2Cl_2$ (Pekov *et al.*, 2023a), evseevite $Na_2Mg(AsO_4)F$ (Pekov *et al.*, 2023b), and magganasite $CuFe^{3+}{}_3O(AsO_4)_3$ (Pekov *et al.*, 2026).

In this paper we describe magnesiohatertite, a member of the alluaudite group within the alluaudite supergroup. This mineral and its name have been accepted by the IMA Commission on New Minerals, Nomenclature and Classification (CNMNC), IMA 2016–078. Magnesiohatertite was approved by the IMA CNMNC with the formula $(Na,Ca)_2Ca(Mg,Fe^{3+})_2(AsO_4)_3$ (Pekov *et al.*, 2016c) and named as a Mg-dominant [in the *M*(2) site] analogue of hatertite for which the IMA-accepted formula in this period was $Na_2(Ca,Na)(Fe^{3+},Cu)_2(AsO_4)_3$ (Krivovichev *et al.*, 2013). The rootname was given in honour of the prominent mineralogist and crystal chemist Professor Frederic Hatert (b. 1974), a well-known specialist in studies of oxysalt minerals including the alluaudite supergroup, who works in University of Liège, Belgium. Later the new nomenclature of the alluaudite supergroup was accepted by the IMA CNMNC (Hatert, 2019), and the idealized formulae of hatertite and magnesiohatertite were redefined as $NaNaCa(CuFe^{3+})(AsO_4)_3$ and $NaNaCa(MgFe^{3+})(AsO_4)_3$, respectively. The IMA-accepted symbol of magnesiohatertite is Mhtt.

The holotype specimen of magnesiohatertite is deposited in the systematic collection of the Fersman Mineralogical Museum of the Russian Academy of Sciences, Moscow with the catalogue number 95622.

Occurrence and General Appearance

The active Arsenatnaya fumarole and its mineralogical features, including zonation in the distribution of mineral associations, were characterized by Pekov *et al.* (2014a, 2018a) and Shchipalkina *et al.* (2020).

Magnesiohatertite was discovered in specimens collected by us in July 2015 from the intermediate (in vertical section of the fumarole) zone located at the depth of about 1.5 m from the day surface. Temperatures measured by us using a chromel-alumel thermocouple in this zone during collecting was 400–420°C. This zone is also characterized by us as the polymineralic zone due to the diversity of mineral species, especially arsenates and sulfates. Magnesiohatertite is associated with sanidine (including the As-bearing variety), fluorophlogopite, hematite, tenorite, cassiterite, pseudobrookite, rutile, johillerite, nickenichite, badalovite, calciojohillerite, bradaczekite, tilasite, svabite, urusovite, lammerite,

Prepublished article

https://doi.org/10.1180/mgm.2026.10218 Published online by Cambridge University Press

paralammerite, ericlaxmanite, popovite, arsmirandite, lehmannite, arsenowagnerite, dmisokolovite, shchurovskyite, yurmarinite, aphthitalite, belomarinaite, metathénardite, langbeinite, calciolangbeinite, anhydrite, krasheninnikovite, euchlorine, wulffite, alumoklyuchevskite, fluoborite, sylvite, halite, and sellaite.

Magnesiohatertite occurs as prismatic crystals, from short prismatic to long prismatic (Figs. 1 and 2), or tabular (flattened presumably on {010}) usually up to 1 mm long and up to 0.3 mm thick, rarely up to 2 mm long and up to 0.5 mm thick. Crystals are coarse (Figs. 1 and 2a), less commonly well-shaped (Fig. 2b), sometimes divergent. The major form observed on tabular crystals is probably the pinacoid {010} while lateral faces were not indiced. They are usually combined in near-parallel or chaotic aggregates (Figs. 1 and 2) up to 0.5 cm across or form interrupted incrustations up to several cm^2 in area overgrowing basalt scoria altered by fumarolic gas. The crystals typically contain abundant inclusions of other arsenates (usually johillerite, calciojohillerite or tilasite), hematite or particles of basalt scoria.

Physical Properties and Optical Data

Magnesiohatertite is grey, greenish-grey, brownish-grey, bluish-grey, pale blue or colourless, rarer pale reddish-brownish. It is transparent or semitransparent, with white streak and vitreous lustre. The mineral is brittle; cleavage or parting was not observed. The fracture is uneven. The Mohs hardness is *ca.* 3½. The density calculated using the empirical formula and unit-cell volume obtained from single-crystal X-ray diffraction data is 4.060 g cm^{-3}.

In plane polarized transmitted light, magnesiohatertite is almost colourless and nonpleochroic in thin grains. In thick grains, it demonstrates distinct pleochroism with the following absorption scheme: *Z* (greyish-bluish) > *Y* (pale greyish-bluish) ~ *X* (pale pinkish-brownish). The mineral is optically biaxial (+), α = 1.728(5), β = 1.745(6), γ = 1.768(6) (589 nm), $2V_{meas.}$ = 85(10)º (estimated by the conoscopical figure on the section perpendicular to the optical axis), and $2V_{calc.}$ = 82º. Dispersion of optical axes is strong, $r < v$. The optical orientation is presumably $Y = b$ (by analogy with other alluaudite-group arsenates).

Raman Spectroscopy

The Raman spectrum of the holotype magnesiohatertite (Fig. 3) was obtained on a randomly oriented crystal using an EnSpectr R532 instrument with a green laser (532 nm) at room temperature. The output power of the laser beam was about 10 mW. The spectrum was processed using the EnSpectr expert mode program in the range from 4000 to 100 cm^{-1} with the use of a holographic diffraction grating with 1800 lines per cm^{-1} and a resolution of 6 cm^{-}

Preprinted article

https://doi.org/10.1180/mgm.2026.10218 Published online by Cambridge University Press

[1]. The diameter of the focal spot on the sample was about 10 μm. The backscattered Raman signal was collected with a 40× objective; signal acquisition time for a single scan of the spectral range was 1500 ms and the signal was averaged over 20 scans.

The Raman spectrum of magnesiohatertite was interpreted according to Nakamoto (1986). The strongest bands in the region 750–900 cm^{-1} correspond to As^{5+}–O stretching vibrations of AsO_4^{3-} anions. Bands with frequencies lower than 500 cm^{-1} correspond to bending vibrations of AsO_4 tetrahedra, Mg–O, Fe–O and Cu–O stretching vibrations and lattice modes. The absence of bands with frequencies higher than 900 cm^{-1} indicates the absence of groups with O–H, C–H, C–O, N–H, N–O and B–O bonds in magnesiohatertite.

Chemical Composition

The chemical composition of magnesiohatertite was determined using a Jeol JSM-6480LV scanning electron microscope equipped with an INCA-Wave 500 wavelength-dispersive spectrometer (Laboratory of Analytical Techniques of High Spatial Resolution, Dept. of Petrology, Moscow State University), with an acceleration voltage of 20 kV, a beam current of 20 nA, and a 10 μm beam diameter; counting time for peak was 10 s and for background 5 s from each side of peak.

The chemical data for the holotype specimen are given in Table 1. Contents of other elements with atomic numbers >6 were below detection limits. The empirical formula calculated on the basis of 12 O atoms per formula unit (*apfu*) is $Na_{1.51}K_{0.16}Ca_{1.06}Mg_{0.89}Mn_{0.06}Cu_{0.51}Zn_{0.21}Al_{0.08}Fe^{3+}_{0.51}(As_{2.97}Si_{0.03}P_{0.02}V_{0.01})_{\Sigma 3.03}O_{12}$. Taking into account the structure data (see below), the simplified formula can be presented as $(Na,Ca,Cu)(Na,K)(Ca,Mn)(Mg,Fe^{3+},Cu,Zn)_2(AsO_4)_3$ and the idealized formula, in accordance with the current nomenclature of the alluaudite group (Hatert, 2019), is $NaNaCa(MgFe^{3+})(AsO_4)_3$.

Electron microprobe analyses of several other specimens of magnesiohatertite from the Arsenatnaya fumarole were given in (Pekov *et al.*, 2018a): see notes below.

X-ray Crystallography and Crystal Structure Determination

The powder X-ray diffraction (XRD) data for the holotype magnesiohatertite (Table 2) were collected with a Rigaku R-AXIS Rapid II single-crystal diffractometer equipped with cylindrical image plate detector (r = 127.4 mm) using Debye-Scherrer geometry, Co$K\alpha$ radiation (rotating anode with VariMAX microfocus optics), 40 kV, 15 mA, and 10 min exposure. Angular resolution of the detector is 0.045º 2Θ (pixel size 0.1 mm). The data were

Prepublished article

https://doi.org/10.1180/mgm.2026.10218 Published online by Cambridge University Press

integrated using the software package osc2Tab (Britvin *et al*., 2017). The unit-cell parameters refined from the powder XRD data are: a = 12.310(8), b = 13.000(3), c = 6.730(5) Å, β = 113.74(4)º, and V = 986(1) Å^3.

Single-crystal X-ray diffraction studies of magnesiohatertite were carried out using a STOE StadiVari diffractometer equipped with a Dectris PILATUS 300K pixel detector. A semiempirical multi-scan absorption correction (SADABS) was applied to the data. The crystal structure was solved by direct methods and refined using the SHELX software package (Sheldrick, 2015). Crystal data, data collection information and structure refinement details are given in Table 3, coordinates and displacement parameters of atoms in Table 4, selected interatomic distances in Table 5, and anisotropic displacement paraments in Table S1.

Discussion

Crystal chemistry

Magnesiohatertite has the alluaudite-type structure which contains seven symmetrically independent cation sites including two tetrahedrally coordinated sites As(1) and As(2) (Tables 4 and 5). They are labeled according to the scheme suggested by Hatert *et al.* (2000) and revisited by Krivovichev *et al.* (2013). The *M*(1) and *M*(2) sites have octahedral coordination. *M*(2) is mix-occupied with prevailing of Mg among divalent cations and Fe^{3+} among trivalent cations. Based on the refined site-scattering factor (e_{ref}, in electrons per site) and *M*(2) – O distances (Tables 4 and 5) and taking into account electron probe data (Table 1), its occupancy was assigned as $Mg_{0.44}Fe^{3+}_{0.26}Cu_{0.18}Zn_{0.12}$. The *M*(1) site is occupied by Ca atoms with an admixture of smaller cations, most likely Mn^{2+}. Two adjacent distorted octahedra $M(2)O_6$ share an edge to form a $[M(2)_2O_{10}]$ dimer. The dimers are linked by the isolated $M(1)O_6$ octahedra forming chains along [-101] (Fig. 4a). $As(1)O_4$ tetrahedra share all vertices with the *M*-centred octahedra to form the (010) heteropolyhedral layers (Fig. 4b) while each $As(2)O_4$ tetrahedron shares three vertices with the MO_6 octahedra of one layer and the fourth vertex with the octahedron of the adjacent layer, thus linking the layers into a three-dimensional framework.

The $A(1)O_6$ and $A(1)'O_4$-centred polyhedra are also a part of the framework (Fig. 4c). The $A(1)O_6$ and $A(1)'O_4$ sites are statistically occupied. The octahedrally coordinated *A*(1) site is Na-dominant (52% of its occupancy) with admixed Ca (30%). The *A*(1)' site, centering slightly twisted square, hosts Cu^{2+} (18%) only when the adjacent *A*(1) site is vacant (Fig. 5). The *A*(1)' position is typical for Cu^{2+} accommodation in the alluaudite-type arsenates

Preprint article

https://doi.org/10.1180/mgm.2026.10218 Published online by Cambridge University Press

(Krivovichev *et al.*, 2013; Hatert, 2019); in magnesiohatertite, the presence of Cu^{2+} atoms at this site is confirmed by the *A*(1)' – O distances ranging from 1.85 to 2.14 Å (Table 4).

The *A*(2)' site, predominantly occupied by Na atoms (88%) with admixed K atoms (12%), is located in channels of the framework (Fig. 4c).

The averaged empirical and simplified (generalized to major constituents) structural formulae of magnesiohatertite are $Na_{1.51}K_{0.16}Ca_{1.06}Mg_{0.89}Mn_{0.06}Cu_{0.51}Zn_{0.21}Al_{0.08}Fe^{3+}_{0.51}(As_{2.97}Si_{0.03}P_{0.02}V_{0.01})_{\Sigma 3.03}O_{12}$ and $^{A(1)}(Na_{0.52}Ca_{0.30}\square_{0.18})^{A(1)'}(\square_{0.82}Cu_{0.18})^{A(2)'}(Na_{0.88}K_{0.12})^{M(1)}(Ca_{0.93}Mn_{0.07})^{M(2)}(Mg_{0.88}Fe^{3+}_{0.52}Cu_{0.36}Zn_{0.24})(AsO_4)_3$, respectively.

In contrast with magnesiohatertite, hatertite was originally described as a Mg-free mineral (*i.e.*, content of Mg is below the detection limit by electron microprobe), and its empirical formula and simplified structural formula are $Na_{1.72}K_{0.32}Ca_{0.78}Mn_{0.14}Cu_{0.64}Zn_{0.16}Al_{0.26}Fe^{3+}_{0.88}As_{3.03}O_{12}$ and $^{A(1)}(Na_{0.87}Ca_{0.13})^{A(1)'}\square^{A(2)'}(Na_{0.55}K_{0.30})^{M(1)}(Ca_{0.60}Na_{0.27}Mn_{0.13})^{M(2)}(Fe^{3+}_{0.90}Cu_{0.40}Al_{0.38}Zn_{0.32})(AsO_4)_3$, respectively (Krivovichev *et al.*, 2013). Note, all our analyses of "hatertite" published in the paper (Pekov *et al.*, 2018a: nos. 52–57 in Table S1) were assigned to hatertite based on "old" nomenclature scheme in which hatertite was considered as a Fe^{3+}-dominant [for *M*(2)] species with the simplified formula $Na_2(Ca,Na)(Fe^{3+},Cu)_2(AsO_4)_3$ while magnesiohatertite as a Mg-dominant [for *M*(2)] mineral with the simplified formula $(Na,Ca)_2Ca(Mg,Fe^{3+})_2(AsO_4)_3$. Using the current IMA-approved nomenclature approach based on the rule of a valency-imposed double-site occupancy for the *M*(2) site [$M^{2+}M^{3+}$] (Hatert and Burke, 2021; Hatert, 2019), we see that these analyses now correspond to magnesiohatertite, ideally $NaNaCa(MgFe^{3+})(AsO_4)_3$, except of analysis no. 56 which corresponds to calciohatertite, ideally $NaNaCa(CaFe^{3+})(AsO_4)_3$ (IMA_2021-013, Koshlyakova *et al.*, 2021) Thus, in this table only the analysis no. 51 cited from Krivovichev *et al.* (2013) corresponds to hatertite in the frame of the current nomenclature of the alluaudite group.

Notes on origin

Magnesiohatertite is a fumarolic mineral formed at temperatures definitely not lower than 450ºC. It can crystallize directly from the gas phase as a volcanic sublimate, however, we consider more probable that it was formed as a result of the interaction between fumarolic gas and basalt scoria. The latter could be a source of Mg and Ca which have very low volatilities in such post-volcanic systems at temperatures up to 400–500°C (Symonds and Reed, 1993).

Pre-published article

https://doi.org/10.1180/mgm.2026.10218 Published online by Cambridge University Press

Acknowledgements

We thank three anonymous referees for their valuable comments. The mineralogical and spectroscopic studies were supported by the Russian Science Foundation, grant no. 25-17-00005 (IVP and MFV). The powder XRD study was performed at the Center for X-Ray Diffraction Research of the Science Park of St. Petersburg State University within the framework of project 125021702335-5.

References

Britvin S.N., Dolivo-Dobrovolsky D.V. and Krzhizhanovskaya M.G. (2017) Software for processing the X-ray powder diffraction data obtained from the curved image plate detector of Rigaku RAXIS Rapid II diffractometer. *Zapiski Rossiiskogo Mineralogicheskogo Obshchestva*, **146(3)**, 104–107 (in Russian).

Hatert F. (2019) A new nomenclature scheme for the alluaudite supergroup. *European Journal of Mineralogy*, **31**, 807–822.

Hatert F. and Burke E.A.J. (2008) The IMA-CNMNC dominant-constituent rule revisited and extended. *The Canadian Mineralogist*, **46**, 717–728.

Hatert F., Keller P., Lissner F., Antenucci D. and Fransolet A.-M. (2000) First experimental evidence of alluaudite-like phosphates with high Li-content: The $(Na_{1-x}Li_x)MnFe_2(PO_4)_3$ series (x = 0 to 1). *European Journal of Mineralogy*, **12**, 847–857.

Koshlyakova N.N., Pekov I.V., Belakovskiy D.I., Vigasina M.F., Zubkova N.V., Agakhanov A.A., Britvin S.N., Sidorov E.G. and Pushcharovsky D.Y. (2021) Calciohatertite, IMA 2021-013. CNMNC Newsletter 62, pp. 634–635. *Mineralogical Magazine*, **85**, 634–638.

Krivovichev S.V., Vergasova L.P., Filatov S.K., Rybin D.S., Britvin S.N. and Ananiev V.V. (2013) Hatertite, $Na_2(Ca,Na)(Fe^{3+},Cu)_2(AsO_4)_3$, a new alluaudite-group mineral from Tolbachik fumaroles, Kamchatka peninsula, Russia. *European Journal of Mineralogy*, **25**, 683–691.

Nakamoto K. (1986) *Infrared and Raman Spectra of Inorganic and Coordination Compounds*. John Wiley & Sons, New York.

Pekov I.V., Zubkova N.V., Yapaskurt V.O., Belakovskiy D.I., Lykova I.S., Vigasina M.F., Sidorov E.G. and Pushcharovsky D.Yu. (2014a) New arsenate minerals from the Arsenatnaya fumarole, Tolbachik volcano, Kamchatka, Russia. I. Yurmarinite, $Na_7(Fe^{3+},Mg,Cu)_4(AsO_4)_6$. *Mineralogical Magazine*, **78**, 905–917.

Pekov I.V., Zubkova N.V., Yapaskurt V.O., Belakovskiy D.I., Vigasina M.F., Sidorov E.G. and Pushcharovsky D.Yu. (2014b) New arsenate minerals from the Arsenatnaya fumarole,

Preprinted article

https://doi.org/10.1180/mgm.2026.10218 Published online by Cambridge University Press

Tolbachik volcano, Kamchatka, Russia. II. Ericlaxmanite and kozyrevskite, two natural modifications of $Cu_4O(AsO_4)_2$. *Mineralogical Magazine*, **78**, 1527–1543.

Pekov I.V., Zubkova N.V., Yapaskurt V.O., Belakovskiy D.I., Vigasina M.F., Sidorov E.G. and Pushcharovsky D.Yu. (2015a) New arsenate minerals from the Arsenatnaya fumarole, Tolbachik volcano, Kamchatka, Russia. III. Popovite, $Cu_5O_2(AsO_4)_2$. *Mineralogical Magazine*, **79**, 133–143.

Pekov I.V., Zubkova N.V., Belakovskiy D.I., Yapaskurt V.O., Vigasina M.F., Sidorov E.G. and Pushcharovsky D.Yu. (2015b) New arsenate minerals from the Arsenatnaya fumarole, Tolbachik volcano, Kamchatka, Russia. IV. Shchurovskyite, $K_2CaCu_6O_2(AsO_4)_4$, and dmisokolovite, $K_3Cu_5AlO_2(AsO_4)_4$. *Mineralogical Magazine*, **79**, 1737–1753.

Pekov I.V., Yapaskurt V.O., Britvin S.N., Zubkova N.V., Vigasina M.F. and Sidorov E.G. (2016a) New arsenate minerals from the Arsenatnaya fumarole, Tolbachik volcano, Kamchatka, Russia. V. Katiarsite, $KTiO(AsO_4)$. *Mineralogical Magazine*, **80**, 639–646.

Pekov I.V., Zubkova N.V., Yapaskurt V.O., Polekhovsky Yu.S., Vigasina M.F., Belakovskiy D.I., Britvin S.N., Sidorov E.G. and Pushcharovsky D.Yu. (2016b) New arsenate minerals from the Arsenatnaya fumarole, Tolbachik volcano, Kamchatka, Russia. VI. Melanarsite, $K_3Cu_7Fe^{3+}O_4(AsO_4)_4$. *Mineralogical Magazine*, **80**, 855–867.

Pekov I.V., Lykova I.S., Koshlyakova N.N., Belakovskiy D.I., Vigasina M.F., Agakhanov A.A., Britvin S.N., Turchkova A.G., Sidorov E.G. and Giester G. (2016c) Magnesiohatertite, IMA 2016-078. CNMNC Newsletter No. 34, December 2016, page 1319; *Mineralogical Magazine*, **80**, 1315–1321.

Pekov I.V., Yapaskurt V.O., Belakovskiy D.I., Vigasina M.F., Zubkova N.V. and Sidorov E.G. (2017) New arsenate minerals from the Arsenatnaya fumarole, Tolbachik volcano, Kamchatka, Russia. VII. Pharmazincite, $KZnAsO_4$. *Mineralogical Magazine*, **81**, 1001–1008.

Pekov I.V., Koshlyakova N.N., Zubkova N.V., Lykova I.S., Britvin S.N., Yapaskurt V.O., Agakhanov A.A., Shchipalkina N.V., Turchkova A.G. and Sidorov E.G. (2018a) Fumarolic arsenates – a special type of arsenic mineralization. *European Journal of Mineralogy*, **30**, 305–322.

Pekov I.V., Zubkova N.V., Agakhanov A.A., Yapaskurt V.O., Chukanov N.V., Belakovskiy D.I., Sidorov E.G. and Pushcharovsky D.Yu. (2018b) New arsenate minerals from the Arsenatnaya fumarole, Tolbachik volcano, Kamchatka, Russia. VIII. Arsenowagnerite, $Mg_2(AsO_4)F$. *Mineralogical Magazine*, **82**, 877–888.

Prepublished article

https://doi.org/10.1180/mgm.2026.10218 Published online by Cambridge University Press

Pekov I.V., Zubkova N.V., Agakhanov A.A., Belakovskiy D.I., Vigasina M.F., Yapaskurt V.O., Sidorov E.G., Britvin S.N. and Pushcharovsky D.Y. (2019a) New arsenate minerals from the Arsenatnaya fumarole, Tolbachik volcano, Kamchatka, Russia. IX. Arsenatrotitanite, $NaTiO(AsO_4)$. *Mineralogical Magazine*, **83**, 453–458.

Pekov I.V., Zubkova N.V., Agakhanov A.A., Ksenofontov D.A., Pautov L.A., Sidorov E.G., Britvin S.N., Vigasina M.F. and Pushcharovsky D.Yu. (2019b) New arsenate minerals from the Arsenatnaya fumarole, Tolbachik volcano, Kamchatka, Russia. X. Edtollite, $K_2NaCu_5Fe^{3+}O_2(AsO_4)_4$, and alumoedtollite, $K_2NaCu_5AlO_2(AsO_4)_4$. *Mineralogical Magazine*, **83**, 485–495.

Pekov I.V., Lykova I.S., Yapaskurt V.O., Belakovskiy D.I., Turchkova A.G., Britvin S.N., Sidorov E.G. and Scheidl K.S. (2019c) New arsenate minerals from the Arsenatnaya fumarole, Tolbachik volcano, Kamchatka, Russia. XI. Anatolyite, $Na_6(Ca,Na)(Mg,Fe^{3+})_3Al(AsO_4)_6$. *Mineralogical Magazine*, **83**, 633–638.

Pekov I.V., Lykova I.S., Agakhanov A.A., Belakovskiy D.I., Vigasina M.F., Britvin S.N., Turchkova A.G., Sidorov E.G. and Scheidl K.S. (2019d) New arsenate minerals from the Arsenatnaya fumarole, Tolbachik volcano, Kamchatka, Russia. XII. Zubkovaite, $Ca_3Cu_3(AsO_4)_4$. *Mineralogical Magazine*, **83**, 879–886.

Pekov I.V., Zubkova N.V., Koshlyakova N.N., Agakhanov A.A., Belakovskiy D.I., Vigasina M.F., Yapaskurt V.O., Britvin S.N., Turchkova A.G., Sidorov E.G. and Pushcharovsky D.Y. (2020a) New arsenate minerals from the Arsenatnaya fumarole, Tolbachik volcano, Kamchatka, Russia. XIII. Pansnerite, $K_3Na_3Fe^{3+}{}_6(AsO_4)_8$. *Mineralogical Magazine*, **84**, 143–151.

Pekov I.V., Koshlyakova N.N., Agakhanov A.A., Zubkova N.V., Belakovskiy D.I., Vigasina M.F., Turchkova A.G., Sidorov E.G. and Pushcharovsky D.Yu. (2020b) New arsenate minerals from the Arsenatnaya fumarole, Tolbachik volcano, Kamchatka, Russia. XIV. Badalovite, $NaNaMg(MgFe^{3+})(AsO_4)_3$, a member of the alluaudite group. *Mineralogical Magazine*, **84**, 616–622.

Pekov I.V., Koshlyakova N.N., Agakhanov A.A., Zubkova N.V., Belakovskiy D.I., Vigasina M.F., Turchkova A.G., Sidorov E.G., Pushcharovsky D.Yu. (2021a) New arsenate minerals from the Arsenatnaya fumarole, Tolbachik volcano, Kamchatka, Russia. XV. Calciojohillerite, $NaCaMgMg_2(AsO_4)_3$, a member of the alluaudite group. *Mineralogical Magazine*, **85**, 215–223.

Pekov I.V., Zubkova N.V., Agakhanov A.A., Yapaskurt V.O., Belakovskiy D.I., Vigasina M.F., Britvin S.N., Turchkova A.G., Sidorov E.G. and Pushcharovsky D.Yu. (2021b) New

Prepublished article

https://doi.org/10.1180/mgm.2026.10218 Published online by Cambridge University Press

arsenate minerals from the Arsenatnaya fumarole, Tolbachik volcano, Kamchatka, Russia. XVI. Yurgensonite, $K_2SnTiO_2(AsO_4)_2$, the first natural tin arsenate, and the katiarsite–yurgensonite isomorphous series. *Mineralogical Magazine*, **85**, 698–707.

Pekov I.V., Koshlyakova N.N., Belakovskiy D.I., Vigasina M.F., Zubkova N.V., Agakhanov A.A., Britvin S.N., Sidorov E.G., Pushcharovsky D.Yu. (2022a) New arsenate minerals from the Arsenatnaya fumarole, Tolbachik volcano, Kamchatka, Russia. XVII. Paraberzeliite, $NaCaCaMg_2(AsO_4)_3$, an alluaudite-group member dimorphous with berzeliite. *Mineralogical Magazine*, **86**, 103–111.

Pekov I.V., Koshlyakova N.N., Belakovskiy D.I., Vigasina M.F., Zubkova N.V., Agakhanov A.A., Britvin S.N., Sidorov E.G. and Pushcharovsky D.Yu. (2022b) New arsenate minerals from the Arsenatnaya fumarole, Tolbachik volcano, Kamchatka, Russia. XVIII. Khrenovite, $Na_3Fe^{3+}{}_2(AsO_4)_3$, the sodium-richest alluaudite-group member. *Mineralogical Magazine*, **86**, 897–902.

Pekov I.V., Zubkova N.V., Agakhanov A.A., Yapaskurt V.O., Belakovskiy D.I., Britvin S.N., Sidorov E.G., Kutyrev A.V. and Pushcharovsky D.Yu. (2023a) New arsenate minerals from the Arsenatnaya fumarole, Tolbachik volcano, Kamchatka, Russia. XIX. Axelite, $Na_{14}Cu_7(AsO_4)_8F_2Cl_2$. *Mineralogical Magazine*, **87**, 109–117.

Pekov I.V., Zubkova N.V., Agakhanov A.A., Vigasina M.F., Yapaskurt V.O., Britvin S.N., Turchkova A.G., Sidorov E.G., Zhitova E.S. and Pushcharovsky D.Yu. (2023b) New arsenate minerals from the Arsenatnaya fumarole, Tolbachik volcano, Kamchatka, Russia. XX. Evseevite, $Na_2Mg(AsO_4)F$, the first natural arsenate with antiperovskite structure . *Mineralogical Magazine*, **87**, 839–848.

Pekov I.V., Zubkova N.V., Agakhanov A.A., Koshlyakova N.N., Chukanov N.V., Yapaskurt V.O., Britvin S.N., Turchkova A.G., Zhitova E.S. and Pushcharovsky D.Yu. (2026) New arsenate minerals from the Arsenatnaya fumarole, Tolbachik volcano, Kamchatka, Russia. XXI. Magganasite, $CuFe^{3+}{}_3O(AsO_4)_3$ // Miner. Mag., **90**, in press. DOI: 10.1180/mgm.2025.10141

Shchipalkina N.V., Pekov I.V., Koshlyakova N.N., Britvin S.N., Zubkova N.V., Varlamov D.A. and Sidorov E.G. (2020) Unusual silicate mineralization in fumarolic sublimates of the Tolbachik volcano, Kamchatka, Russia – Part 1: Neso-, cyclo-, ino- and phyllosilicates. *European Journal of Mineralogy*, **32**, 101–119.

Sheldrick G.M. (2015) Crystal structure refinement with SHELXL. *Acta Crystallographica*, **C71**, 3–8.

Preprint published article

https://doi.org/10.1180/mgm.2026.10218 Published online by Cambridge University Press

Symonds R.B. and Reed M.H. (1993) Calculation of multicomponent chemical equilibria in gas-solid-liquid systems: calculation methods, thermochemical data, and applications to studies of high-temperature volcanic gases with examples from Mount St. Helens. *American Journal of Science*, **293**, 758–864.

Table 1. Chemical composition (wt. %) of the holotype magnesiohatertite.

Constituent	Average*	Range	Standard Deviation	Probe Standard
Na_2O	7.76	7.49 – 8.09	0.28	jadeite
K_2O	1.25	1.03 – 1.53	0.22	$KTiOPO_4$
CaO	9.84	7.73 – 11.59	1.54	$CaSiO_3$
MgO	5.93	5.22 – 6.96	0.66	olivine
MnO	0.70	0.66 – 0.74	0.03	$MnTiO_3$
CuO	6.78	4.39 – 9.79	2.26	Cu
ZnO	2.85	2.02 – 3.47	0.62	ZnS
Al_2O_3	0.64	0.46 – 0.87	0.16	jadeite
Fe_2O_3**	6.76	5.27 – 7.83	1.08	FeS_2
TiO_2	0.02	0.00 – 0.07	0.02	$KTiOPO_4$
SiO_2	0.25	0.04 – 0.65	0.25	jadeite
P_2O_5	0.25	0.21 – 0.31	0.04	$KTiOPO_4$
V_2O_5	0.10	0.07 – 0.14	0.03	V
As_2O_5	56.71	55.65 – 57.31	0.65	GaAs
SO_3	0.02	0.00 – 0.07	0.02	ZnS
Total	99.86			

*Averaged for five spot analyses.
**Fe is considered as Fe^{3+} due to the structure data (see below) and taking into account the extremely oxidizing conditions of mineral deposition in the Arsenatnaya fumarole (Pekov *et al.*, 2018a; Shchipalkina *et al.*, 2020).

Preprint article

https://doi.org/10.1180/mgm.2026.10218 Published online by Cambridge University Press

Table 2. Powder X-ray diffraction data of magnesiohatertite.

I_{obs}	d_{obs}, Å	I_{calc}*	d_{calc}, Å**	*h k l*
35	**6.50**	25	6.501	020
5	5.91	4	5.915	-111
26	**5.66**	20	5.631	200
6	4.494	3	4.467	021
15	4.409	8	4.389	111
15	4.285	12	4.256	220
11	4.195	8	4.141	-221
8	4.080	1	4.045	130
12	3.854	14	3.825	-311
41	**3.635**	27, 18	3.630, 3.606	-131, 310
3	3.334	3	3.321	-202
55	**3.221**	52	3.223	-112
27	**3.086**	9, 20	3.086, 3.074	221, 002
23	**2.987**	31	2.979	-312
19	2.949	9, 2	2.957, 2.940	-222, -331
100	**2.837**	7, 49, 100	2.837, 2.815, 2.815	330, 400, 240
57	**2.792**	2, 5, 8	2.781, 2.779, 2.778	-241, 022, -421
13	2.702	1, 17	2.689, 2.686	311, -402
42	**2.648**	18, 26	2.645, 2.639	112, -132
15	2.613	6	2.583	420
6	2.517	3	2.482	-422
2	2.443	1	2.417	-511
4	2.334	3	2.331	202
5	2.301	6, 3, 2, 1	2.323, 2.321, 2.293, 2.281	-242, 331, 132, -512
4	2.237	2	2.233	-441
5	2.205	8	2.219	510
4	2.156	1, 3, 5	2.181, 2.139, 2.138	-351, -531, 350
2	2.114	1	2.118	421
5	2.060	3, 3, 1, 10	2.070, 2.049, 2.044, 2.043	-442, -152, 061, -532
5	2.024	1	2.022	260
8	1.997	2, 3, 4, 12	2.008, 1.999, 1.989, 1.982	-423, 530, 312, -352
7	1.953	1, 2, 4	1.955, 1.946, 1.946	023, -621, -133
5	1.874	10	1.874	152
13	1.833	2, 12	1.833, 1.826	170, 332
3	1.736	1, 2	1.730, 1.730	-552, 133
3	1.724	2, 1, 3, 1	1.727, 1.726, 1.725, 1.722	531, -623, 171, -711
5	1.699	13, 3, 3	1.704, 1.702, 1.693	-642, 550, 422
8	1.665	1, 1, 18	1.669, 1.666, 1.663	-153, -314, -204
1	1.584	6	1.588	-372
4	1.569	1, 3	1.573, 1.571	621, 081
6	1.555	1, 2, 6	1.557, 1.557, 1.556	461, -263, -281
9	1.544	3, 5, 8	1.543, 1.539, 1.536	442, 371, -802
6	1.523	2, 2	1.525, 1.520	551, -733
7	1.490	3	1.495	-822

Republished article

https://doi.org/10.1180/mgm.2026.10218 Published online by Cambridge University Press

4	1.468	5, 1	1.475, 1.472	281, -821
3	1.458	1, 1	1.463, 1.454	333, 532
1	1.447	1, 4	1.449, 1.448	-572, -752
1	1.434	1, 2, 3, 1, 1	1.437, 1.434, 1.433, 1.433, 1.430	-481, -823, 570, 190, -714
3	1.422	5	1.423	-373
2	1.407	5, 1	1.408, 1.407	800, 480
5	1.392	1, 9, 1	1.391, 1.390, 1.389	-482, 044, -842
8	1.357	1, 2, 9, 5, 1	1.360, 1.351, 1.351, 1.348, 1.348	-912, 731, 204, -573, 390
3	1.334	2, 1	1.339, 1.333	-843, 282
2	1.328	4	1.327	552
2	1.283	1, 1	1.288, 1.280	-483, -335

*For the calculated pattern, only reflections with intensities ≥1 are given; **for the unit-cell parameters obtained from single-crystal data; the strongest reflections are marked in bold type.

Table 3. Crystal data, data collection information and structure refinement details for magnesiohatertite.

Crystal chemical formula	$(Na_{0.52}Ca_{0.30}\square_{0.18})(\square_{0.82}Cu_{0.18})(Na_{0.88}K_{0.12})(Ca_{0.93}Mn_{0.07})(Mg_{0.88}Fe^{3+}_{0.52}Cu_{0.36}Zn_{0.24})(AsO_4)_3$
Crystal system, space group, *Z*	Monoclinic, *C*2/*c*, 4
a, Å	12.3098(10)
b, Å	13.0021(11)
c, Å	6.7211(5)
β, °	113.823(4)
V, Å^3	984.08(14)
λ (Mo*K*a) (Å), *T* (K)	0.71073, 293(2)
Crystal size (mm)	0.015 × 0.025 × 0.040
Diffractometer	STOE StadiVari
θ range (°)	3.13–28.28
h, *k*, *l* range	-16 ≤ *h* ≤ 16, -17 ≤ *k* ≤ 17, -8≤ *l* ≤ 8
Reflections collected	8875
Unique reflections, R_{int}	1213, 0.045
Reflections with $I > 2\sigma(I)$	1109
Number of refined parameters	108
*R*1	0.033
w$R2_{all}$ (F^2)	0.075
GoF	1.12
$\Delta\rho_{max}$ /$\Delta\rho_{min}$ (e/Å^3)	1.54/-1.14

Preprint not peer reviewed

https://doi.org/10.1180/mgm.2026.10218 Published online by Cambridge University Press

Table 4. Atom coordinates, equivalent thermal displacement parameters (U_{eq}, Å^2) of atoms, site occupancies and site multiplicities (Q) in the structure of magnesiohatertite.

Site	*x*	*y*	*z*	U_{eq}	Site occupancy	*Q*
A(1)	½	0	0	0.0226(12)	$Na_{0.52(2)}Ca_{0.30(2)}$*	4
A(1)’	0	0.5087(9)	¼	0.074(5)	$Cu_{0.179(8)}$*	4
A(2)’	0	0.9812(3)	¼	0.0296(13)	$Na_{0.88(2)}K_{0.12(2)}$	4
M(1)	0	0.26557(12)	¼	0.0170(4)	$Ca_{0.93(2)}Mn_{0.07(2)}$	4
M(2)	0.77712(8)	0.84274(7)	0.86490(15)	0.0116(3)	$Mg_{0.44}Fe_{0.26}Cu_{0.18}Zn_{0.12}$**	8
As(1)	0.23751(5)	0.89390(4)	0.13041(8)	0.01240(15)	As	8
As(2)	0	0.72147(6)	¼	0.01104(18)	As	4
O(1)	-0.0490(4)	0.7967(3)	0.0283(6)	0.0174(8)	O	8
O(2)	0.8997(4)	0.6390(4)	0.2723(8)	0.0277(10)	O	8
O(3)	0.1703(4)	0.8334(3)	0.8901(6)	0.0175(8)	O	8
O(4)	0.3822(4)	0.9105(3)	0.1914(7)	0.0196(8)	O	8
O(5)	0.2272(4)	0.8209(3)	0.3299(7)	0.0227(9)	O	8
O(6)	0.1668(4)	0.0061(3)	0.1122(7)	0.0224(9)	O	8

**A*(1) and *A*(1)’ are alternatively occupied sites. ***Based on the experimental value of site-scattering factor (e_{ref} = 21.16) and chemical composition obtained by electron probe (Table 1).

Table 5. Selected interatomic distances (Å) in the structure of magnesiohatertite.

M(2)	– O(2)	2.006(5)	*A*(2)’	– O(6)	2.476(4) x 2
	– O(1)	2.061(4)		– O(6)	2.591(5) x 2
	– O(3)	2.066(4)		– O(1)	2.759(5) x 2
	– O(6)	2.068(4)		*– O(3)*	*3.082(5) x 2*
	– O(5)	2.093(4)	<*A*(2)’-O>		2.609
	– O(5)	2.201(5)			
<*M*(2)-O>		2.083	*A*(1)’	– O(4)	1.851(9) x 2
				– O(2)	2.137(10) x 2
M(1)	– O(3)	2.311(4) x 2	<*A*(1)’-O>		1.994
	– O(4)	2.313(4) x 2			
	– O(1)	2.330(4) x 2	As(1)	– O(4)	1.673(4)
<*M*(1)-O>		2.318		– O(6)	1.677(4)
				– O(3)	1.683(4)
A(1)	– O(4)	2.308(4) x 2		– O(5)	1.689(4)
	– O(2)	2.368(4) x 2	<As(1)-O>		1.681
	– O(4)	2.572(4) x 2			
<*A*(1)-O>		2.416	As(2)	– O(1)	1.678(4) x 2
				– O(2)	1.687(4) x 2
			<As(2)-O>		1.683

Preprint not published article

https://doi.org/10.1180/mgm.2026.10218 Published online by Cambridge University Press

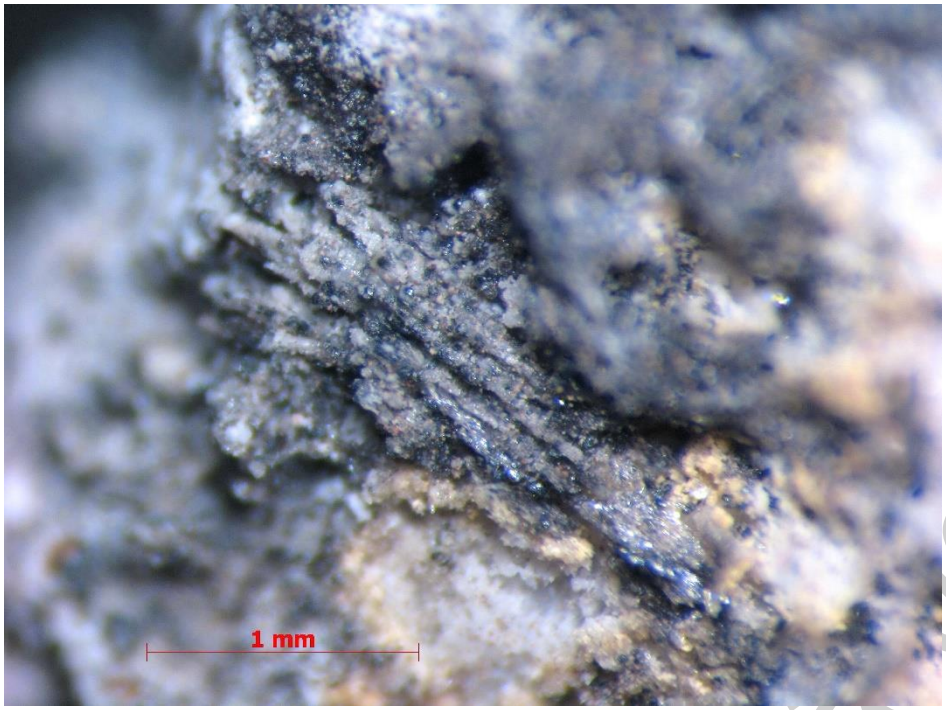

Figure 1. Near-parallel aggregate of grey coarse prismatic crystals of magnesiohatertite with overgrowing small iron-black tenorite crystals on basalt scoria altered to sanidine aggregate by fumarolic gas. FOV width: 3.5 mm. Photo: I.V. Pekov & A.V. Kasatkin.

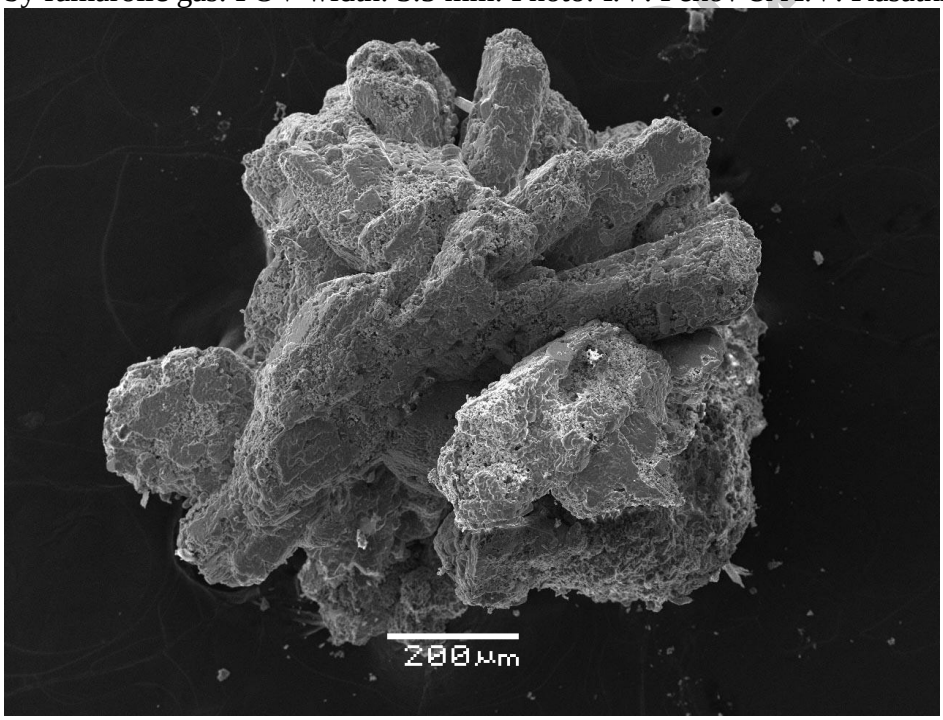

a

https://doi.org/10.1180/mgm.2026.10218 Published online by Cambridge University Press

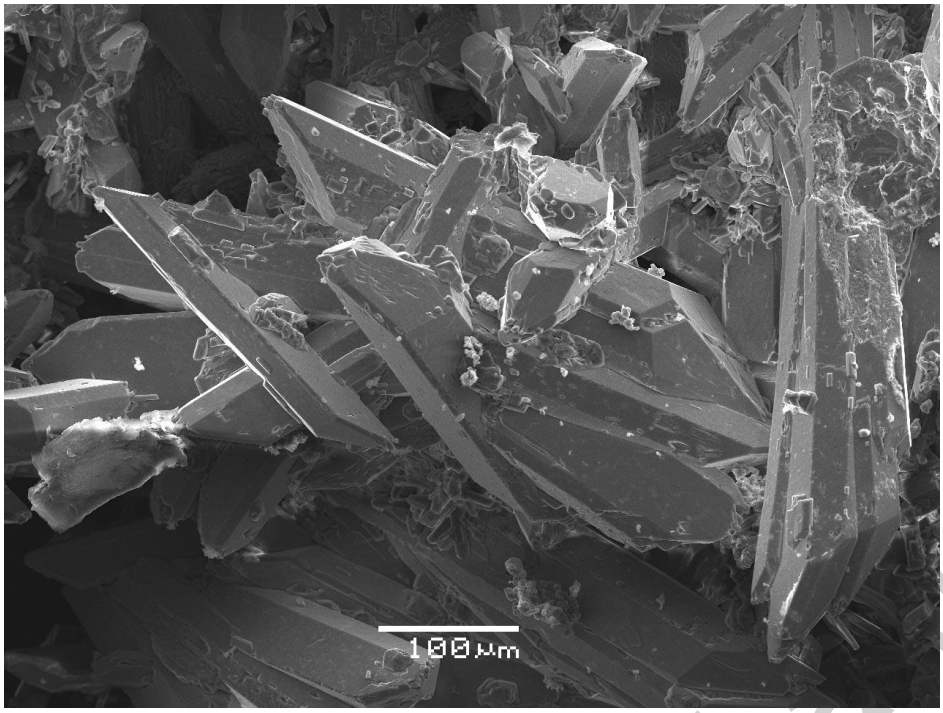

b

Figure 2. Clusters of coarse (a) and well-shaped (b) crystals of magnesiohatertite. SEM (SE) images.

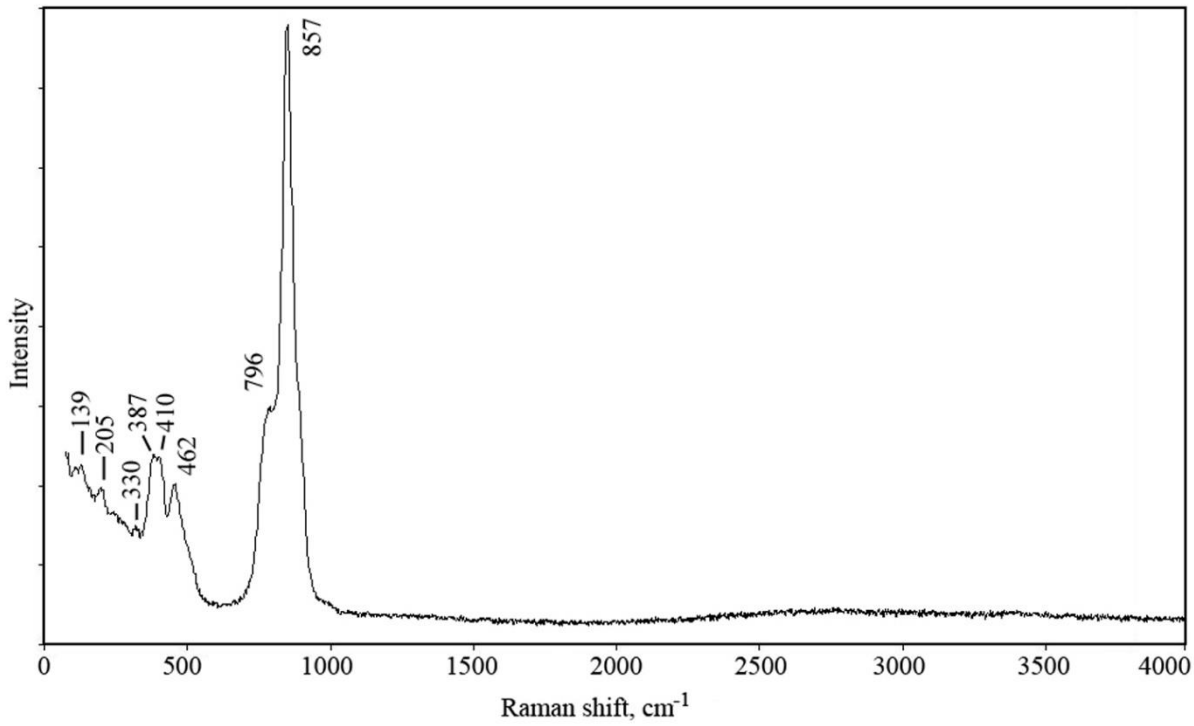

Figure 3. The Raman spectrum of magnesiohatertite.

https://doi.org/10.1180/mgm.2026.10218 Published online by Cambridge University Press

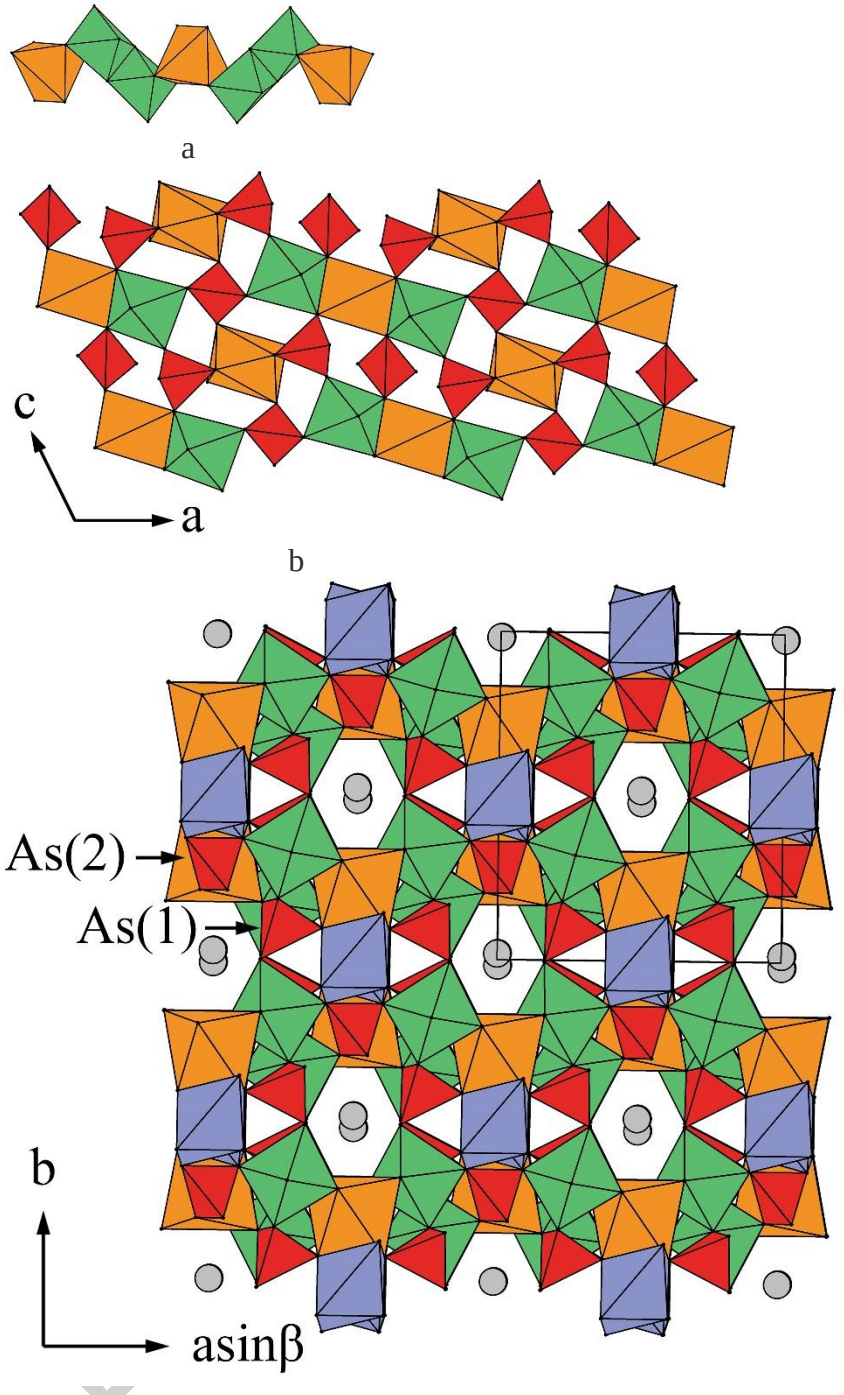

Figure 4. Chains of $M(1)O_6$ [orange] and $M(2)O_6$ [green] octahedra in the structure of magnesiohatertite (a) are linked by AsO_4 tetrahedra [red] forming layers (b) coplanar to (010). The layers are further linked into three-dimensional framework *via* AsO_4 tetrahedra and alternatively occupied $A(1)O_6$ octahedra [purple] and $A(1)'O_4$ squares [are not shown for simplicity, see Fig. 5] with $A(2)'$ site [shown as grey circles] in channels (c). The unit cell is outlined.

https://doi.org/10.1180/mgm.2026.10218 Published online by Cambridge University Press

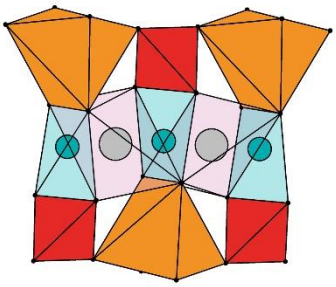

Figure 5. Alternatively occupied $A(1)O_6$ octahedra [transparent purple] and $A(1)'O_4$ squares [transparent blue] link neighboring layers (see Fig. 4b) in the structure of magnesiohatertite. AsO_4 tetrahedra are red, $M(1)O_6$ octahedra are orange.

Prepublished article

https://doi.org/10.1180/mgm.2026.10218 Published online by Cambridge University Press